# Left atrial appendage automatic segmentation, in computed tomography images

# Left atrial appendage automatic segmentation, in computed tomography images

**Y Huérfano[1], M Vera[2], M I Vera[1], O Valbuena[2], E Gelvez-Almeida[2], J Salazar-Tores[2], and V Molina[3]**
[1] Universidad de Los Andes, San Cristóbal, Venezuela
[2] Universidad Simón Bolívar, San José de Cúcuta, Colombia
[3] Universidad ECCI, Bogotá, Colombia

E-mail: m.avera@unisimonbolivar.edu.co

**Abstract**. The left atrial appendage is one of the anatomical places where most frequently blood thrombi occur. When migrating from the appendage, these thrombi, become blood emboli that, potentially, can compromise the physiology and/or anatomy of cardiac or cerebral blood vessels, being able to generate cerebrovascular events. The left atrial appendage segmentation is very difficult due, mainly, to its location and the identical densitometric information presents into of this appendage and around of the left atrium. In this paper, an automatic technique is proposed to segment this appendage with the purpose of generating important information to the procedure called left atrial appendage surgical closure. This information is linked to the volume and the diameters of the left atrial appendage. The technique consists of a digital pre-processing stage, based on filtering processes and definition of a region of interest and, of one segmentation stage that considers a clustering method. The results are promising and they allow us to calculate useful quantitative variables when characterizing the most lethal appendix of the human body represented by the mentioned appendage. These results are very important in clinical processes where both the shape and volume of this appendage are vital for detecting and monitoring some vascular diseases such as cardiac embolism, arterial hypertension and stroke, among others.

## 1. Introduction

In this paper, the morphology of left atrial appendage (LAA) is classified taking into account the paper of Koplay *et al*. [1]. Considering the LAA´s apex initial orientation, the left atrial appendage morphology can be classified in three shapes: wing, long finger and short finger.

Additionally, Figure 1 shows the main medical imaging modalities used for diagnosis of several human pathologies. An example of these pathologies is the left atrial fibrillation (LAF) which is strongly linked to anatomy and physiology of LAA [2]. Frequently, LAF produces cardiac embolism and a very high percentage of cardiac emboli is generated by LAA [3].

In this investigation, we chose multi-slice computed tomography (MSCT) modality to generate the LAA morphology and to obtain very important quantitative LAA's parameters used in surgical routine such as the diameters and volume of LAA [3].

Several researchers have developed computational models to generate the LAA segmentation using approaches with the purpose of: a) detecting atrial fibrillation [4,5] and b) developing percutaneous LAA closure [6,7].

In our paper, we use MSCT images and propose a computational strategy, based on the application of a filter bank and region growing (RG) technique, for LAA automatic segmentation.

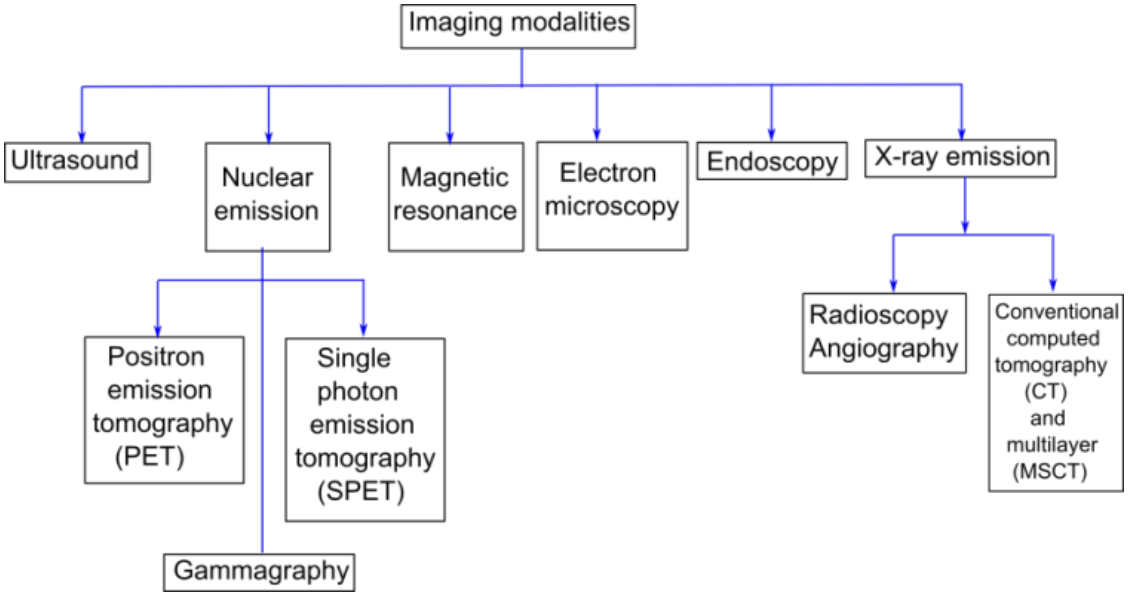


**Figure 1.** Imaging modalities used in the medical routine.

## 2. Materials and methods

### *2.1. Dataset*

One three-dimensional MSCT dataset was used and it was supplied by the Instituto de BioIngeniería y Diagnóstico S.A,, Venezuela. Additionally, LAA manual segmentation (ground truth) generated by a cardiologist, is available.

### *2.2. Computational strategy proposed*

Figure 2 shows a block diagram of the automatic computational strategy (ACS), proposed in this paper, for segmenting the LAA.

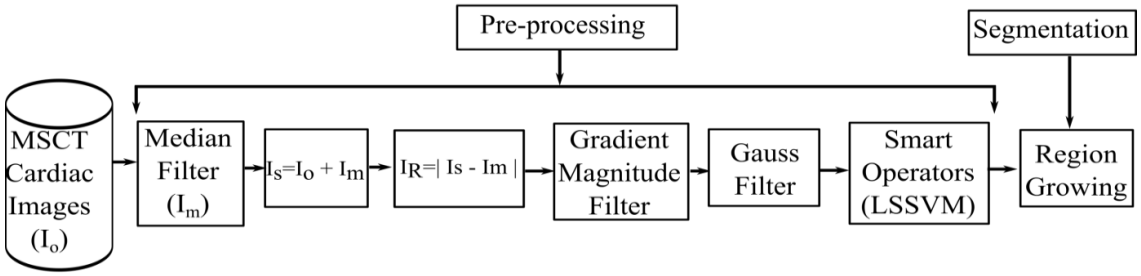


**Figure 2.** Block Diagram of the proposed strategy (ACS).

*2.2.1 Pre-processing.* At this stage, initially, a filter bank is applied to the dataset described in section. Then, a smart operator based on least square support vector machines (LSSVM) is applied in order to define a region of interest. A brief explanation of these filters is found below.

Median filter. This filter computes a smoothed image (Im) of the original image (Io) using the median of an arbitrary neighborhood of each voxel present into Io. The median filter performance is

controlled by two parameters: neighbourhood size (ns), normally between (1x1x1) and (11x11x11), and an arbitrary step size (sz), usually sz belong to the set of natural numbers. In this paper, using the values proposed in [8], an isotropic approach is considered for the ns which is a tuning parameter that varies between (1x1x1) and (7x7x7), with a step size equal to 1. The others ns were not considered because the computational cost, when this filter deal with the considered images, is prohibited.

Arithmetic images. A saturated image (Is) is obtained using the arithmetic addition of Io and Im; whereas an enhanced image ($I_R$) is calculated by the absolute value of the arithmetic subtraction of Is and Im.

Gradient Magnitude filter (GMF). In this work, an approach based on finite differences centered was used for GMF computational implementation [9]. This filter generates a smoothed version, called $I_{GM}$, calculating the three-dimensional gradient magnitude of $I_R$, using the mathematical model given by Equation (1).

$$I_{GM} = \left(\left(\frac{\partial I_R}{\partial i}\right)^2 + \left(\frac{\partial I_R}{\partial j}\right)^2 + \left(\frac{\partial I_R}{\partial k}\right)^2\right)^{1/2} \quad (1)$$

being: i, j, k the spatial directions in which the gradient is calculated and $\left(\frac{\partial I_R}{\partial i}, \frac{\partial I_R}{\partial j}, \frac{\partial I_R}{\partial k}\right)$ the partial derivatives of $I_R$.

The computational cost (time of calculations) of the continuous model for GMF, given by the Equation (1), is very expensive. By this reason an approach based on central finite differences is used, in this paper, for modelling computationally the GMF [10].

Gauss Filter. This filter smooths an image by convolving it with a Gaussian kernel using as standard deviations, the standard deviation of $I_{GM}$ [11]. A discrete Gaussian distribution represented by the mentioned kernel, with arbitrary size, can be used. The kernel values are obtained according to Pascal's triangle. In this research, the size of its kernel is arbitrarily set to (3x3x3). The use of others size Gaussian kernel it is not recommended because it can modify the optimal structure of this kind of filter.

Smart operators: LSSVM for volume of interest definition. Due to the high similarity about densitometric information into both left atrium and the LAA, it is necessary to establish a volume of interest (VOI) in order to address the low contrast problem. A detailed explanation of the how the LSSVM are used in VOI definition, can be found in [12].

*2.2.2 Segmentation.* This stage involves two steps: seed point detection and RG segmentation technique. These steps are presented at next.

Seed point detection. In the dataset, a LSSVM detect the seed voxel using the procedure explained in [13].

Region growing technique (RG). The RG technique applied in this work uses the confidence connected approach for LAA segmentation. In the RG, the coordinates of the seed voxel are necessary. These coordinates are detected using LSSVM ant they are used as the initial position for start growing the initial neighbourhood, which has an arbitrary size (s). The criterion for including new voxels in the region is defined by an intensity range around the mean value of the voxels existing in this region. The extent of the densitometric information interval is computed as the product of the variance image and an arbitrary multiplier (*m*) [13].

During the tuning process, the LAA segmented is compared with the ground truth traced by cardiologists. The Dice score (Ds) is used in order to estimate the difference between these structures [14]. The Ds is a metric with values between zero and 1. This metric is better when its value is closest to 1. Additionally, the areas and perimeters of segmented structures are calculating in order to build a LES characterization.

## 3. Results

A maximum Ds of 0.91 is obtained from the tuning, which generated the optimal parameters for RG technique (m = 6.5 and s = 2). The LSSVM optimal parameters were 0.5 for penalty error parameter and 1.25 for the radial base function deviation parameter; while the best size of median filter was (5x5x5). It represents the optimal value for ns parameter, in this research, which was obtained heuristically. Figure 3 shows an axial view of an original image and the images linked to digital processing developed with the ACS.

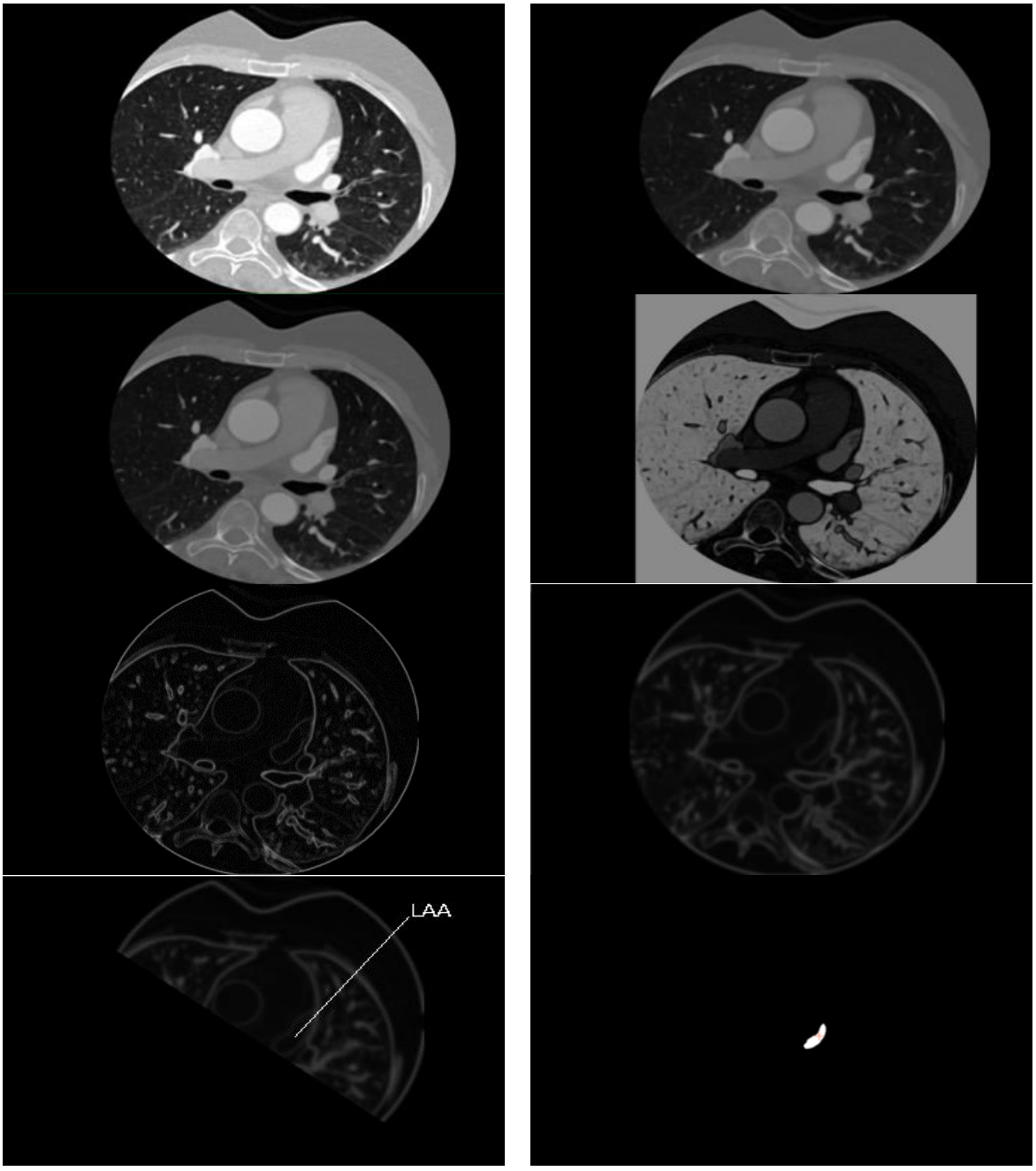


**Figure 3.** Effect of the ACS using a 2D view of LAA. The description will be done considering left to right figure orientation and take into account each image in the rows of this figure. Top row: Original and Median. Second row: Satured and Enhancement. Third row: Gradient and Gauss. Bottom row: VOI for LAA and LAA segmentation.

Additionally, for an improved observation of the three-dimensional morphology of segmented LAA. An amplified version of this appendage is shown in Figure 4.

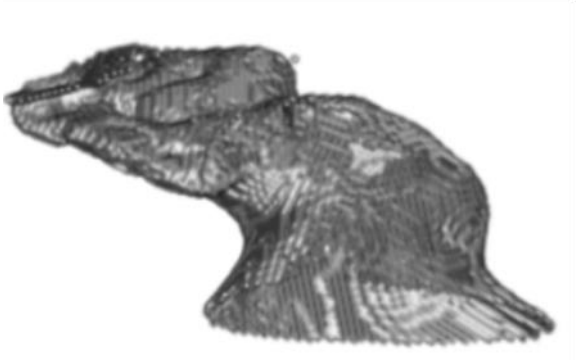

**Figure 4.** Segmented LAA: 3D view.

We can see that the LAA has a wing shape with a wide base. Finally, Table 1 shows the volume values (voxel size multiplied by the number of LAA voxels) and the LAA diameters considering its automatic segmentation.

**Table 1.** Clinical parameters associated with segmented LAA.

| Parameters | LAA |
|---|---|
| Volume ($cm^3$) | 1.08 |
| Smaller diameter (cm) | 1.17 |
| Larger diameter (cm) | 2.44 |

In this section, it is necessary pointed that the Ds is a metric with values between 0 and 1. This metric is better when its value is closest to 1 [14]. In a medical image segmentation context, this means that the manual segmentation and the automatic one matching when the Ds is 1 and they no matching at all when the Ds is zero. In this sense, normally, values of Ds over 0.75 are good accepted, in the medical routine.

According to the results of this paper, the maximum Ds value obtained for the LAA segmentation was 0.91. This value is comparable with Ds = 0.94 obtained in [5]. So, we can say that the ACS, developed in this research, had a good performance segmenting LAA.

## 4. Conclusions

In this paper, a novel automatic strategy for LAA segmentation, identified as ACS, was developed using an adequate group of pre-processing techniques (median, satured, gradient magnitude, Gauss filters and LSSVM operator) and a segmentation technique based on RG.

The considered filters let us address the noise and the artefacts problems; whereas the use of LSSVM, for VOI definition, let us address the low contrast problem, present in MSCT cardiac images.

Additionally, in this research, manual and automatic LAA segmentation were compared and as results the Ds value obtained suggests that the automatic technique developed has a good performance when the LAA segmentation is performed. The LAA segmentation is a crucial step in a surgical procedure called percutaneous LAA closure because this kind of segmentation allows obtaining LAA's parameters such as its volume and diameters.

Finally, it is planned, for the future, to use the ACS in the segmentation of an important number of datasets.

## References

[1] Koplay M, Erol C, Paksoy Y, Kivrak A and Ozbek S 2012 An investigation of the anatomical variations of left atrial appendage by multidetector computed tomographic coronary angiography *Eur. J. Radiol.*

**81(1)** 1575
[2] Go A, Hylek E, Phillips K, Chang Y, Henault L and Selby J 2001 Prevalence of diagnosed atrial fibrillation in adults: national implications for rhythm management and stroke prevention: the anticoagulation and risk factors in atrial fibrillation study *JAMA* **285(1)** 2370
[3] Park J, Bethencourt A, Sievert H, Santoro G, Meier B and Walsh K 2011 Left atrial appendage closure with amplatzer cardiac plug in atrial fibrillation: initial European experience *Catheter Cardiovasc Interv.* **77(1)** 700
[4] Jin C, Feng J, Wang L, Yu H, Liu J, Lu J and Zhou J 2018 Left atrial appendage segmentation and quantitative assisted diagnosis of atrial fibrillation based on fusion of temporal-spatial information *Comput. Biol. Med.* **96(1)** 52
[5] Jin C, Feng J, Wang L, Yu H, Liu J, Lu J and Zhou J 2018 Left atrial appendage segmentation using fully convolutional neural networks and modified three-dimensional conditional random fields *IEEE Journal of Biomedical and Health Informatics* **22(6)** 1906
[6] Morais P, Queirós S, De Meester P and Budts W 2018 Fast segmentation of the left atrial appendage in 3d transesophageal echocardiographic images *IEEE Transactions on Ultrasonics Ferroelectrics and Frequency Control* **65(12)** 2332
[7] Leventic H, Babin D, Velicki L, Devos D, Galic I, Zlokolica V, Romic K and Pižurica A 2019 Left atrial appendage segmentation from 3d ccta images for occluder placement procedure *Comput. Biol. Med.* **104(1)** 163
[8] González R and Woods R 2001 *Digital image processing* (USA: Prentice Hall)
[9] Pratt W 2007 *Digital image processing* (USA: John Wiley & Sons Inc)
[10] Burden R and Faires D 2010 *Numerical analysis* (Mexico: Cengage learning)
[11] Koenderink J 1984 The structure of images *Biol. Cybern.* **50** 363
[12] Vera M, Medina R, Del Mar A, Arellano J, Huérfano Y and Bravo A 2019 An automatic technique for left ventricle segmentation from msct cardiac volumes *J. Phys.: Conf. Ser.* **1160** 012001
[13] Bravo A, Vera M, Garreau M and Medina R 2011 Three–dimensional segmentation of ventricular heart chambers from multi–slice computerized tomography: an hybrid approach *Proc. Digital Information and Communication Technology and Its Applications* (France: Springer) p **166** 287
[14] Dice L 1945 Measures of the amount of ecologic association between species *Ecology* **26(3)** 29